https://doi.org/10.5194/essd-2020-374
Preprint. Discussion started: 17 December 2020

Open Access Earth System Science Data Discussions

University of Nebraska UAS profiling during LAPSE-RATE

Ashraful Islam[1], Ajay Shankar[1], Adam Houston[2], and Carrick Detweiler[1]

[1]Department of Computer Science & Engineering, University of Nebraska-Lincoln, Lincoln, NE 68588, USA.
[2]Department of Earth & Atmospheric Sciences, University of Nebraska-Lincoln, Lincoln, NE 68588, USA.

Correspondence: Ashraful Islam (mislam@huskers.unl.edu)

Abstract.

This paper describes the data collected by the University of Nebraska-Lincoln (UNL) as part of the field deployment during the Lower Atmospheric Process Studies at Elevation — a Remotely-piloted Aircraft Team Experiment (LAPSE-RATE) flight campaign in July 2018. UNL deployed two multirotor unmanned aerial systems (UASs) at various sites in the San Luis Valley (Colorado, USA) for data collection in support of three science missions: convection-initiation, boundary layer transition, and cold air drainage flow. We conducted 172 flights resulting in over 1300 minutes of cumulative flight time. Our novel design for the sensor housing onboard the UAS was employed in these flights to meet the aspiration and shielding requirements of the temperature/humidity sensors, and attempt to separate them from the mixed turbulent airflow from the propellers. Data presented in this paper include time-stamped temperature and humidity data collected from the sensors, along with the three-dimensional position and velocity of the UAS. Data are quality controlled and time-synchronized using a zero-order-hold interpolation without additional post processing. The full dataset is also made available for download at (https://doi.org/10.5281/zenodo.4306086 (Islam *et al.* , 2020)).

1 Introduction

Multirotor UASs are finding more routine uses for sampling and profiling the atmospheric boundary layer (ABL) (Elston *et al.*, 2015; Bonin *et al.*, 2013). UASs enable such profiling with a greater frequency, increased spatio-temporal resolution of data, and in virtually any sampling location when compared with traditional methods. Multirotors extend this capability by allowing rapid and repeatable fixed-site profiling. Our previous work (Islam *et al.* , 2019) describes the design and evaluation of a temperature-humidity (TH) sensor housing that meets the recommended sensor placement, aspiration and shielding criteria by using a passively induced-airflow technique. The sensor housing design has evolved over multiple design iterations and has been field tested in multiple CLOUD-MAP field campaigns (Jacob *et al.*, 2018; Houston *et al.*, 2018).

Two primary highlights of the novel sensor housing are the ability to reliably obtain sensor reading during both ascent and descent profiles, and its invariance to the aircraft orientation relative to ambient wind. Two key design considerations to achieve these goals are: placement of the sensor and consistent aspiration. Placement of the sensor on UAS body can adversely affect the measurements (Greene *et al.*, 2018; Jacob *et al.*, 2018). According to experimental results presented by (Villa *et al.*, 2016), the validity of the measurement increases farther away from the propeller. More specifically from (Prudden *et al.*, 2016), sensors placed at least 2.5× the propeller diameter away from the rotor experiences significantly less propeller interference. Consistent

https://doi.org/10.5194/essd-2020-374
Preprint. Discussion started: 17 December 2020

Figure 1. UAS setup with temperature-humidity sensor mounted in aspirated and shielded sensor housing.

and sufficient aspiration is also necessary for consistent effective sensor response time (Houston and Keeler, 2018). Placing the sensor inside the propeller region or near the body can result in inconsistent aspiration due to rotor turbulence (Ventura Diaz and Yoon, 2018; Yoon *et al.*, 2017). As such, we designed our sensor housing to source the sampling air from outside rotor interference, and to maintain consistently high aspiration air speed to obtain reliable results. Detailed description of the sensor housing design along with the verification of data are available in the open access paper (Islam *et al.* , 2019).

For the LAPSE-RATE campaign, UNL deployed two identical UASs with one primary sensor suite for measurements, and a secondary sensor suite for redundancy and testing. Figure 1 shows a picture of the UAS with the housing setup. Both sensors are located inside their respective sensor housings mounted on two diametrically opposing arms of the UAS. In some flights a third sensor was mounted *under* the body-center of the UAS to compare the performance of primary sensors against traditional mounting positions. A detailed description of our configuration is presented in Section 2.5.

UNL deployed the UASs in five locations in San Luis Valley (Colorado, USA), through 15-19 July 2018. The maximum flight altitude for each flight ranged from 100 - 500 m above ground level. We conducted 172 flights over a span of 4 days. The rest of the paper describes the systems, flight strategies, data processing and quality controls and sample of the data.

2 System Description

2.1 UAS platform

The two identical UASs deployed during the missions were developed on a *DJI Matrice 600Pro* platform equipped with *DJI A3 Pro* flight control systems. Unfolded dimensions (including propellers, frame arms, GPS mounts, and landing gear) of the system are $1668mm \times 1518mm \times 727mm$. The recommended maximum payload capacity of the platform is 5.5 kg. At no load, the UAS has a flight endurance of 35–40 min on a single set of six DJI TB48S batteries. The manufacturer-specified positioning accuracy is $\pm 0.5\mathrm{m}$ in the vertical axis, and ± 1.5 m horizontal (DJI , 2019). The maximum ascent and descent speeds are 5 m/s and 3 m/s, respectively. The flight controller offers real-time access to UAS's on-board sensor data, such as

https://doi.org/10.5194/essd-2020-374
Preprint. Discussion started: 17 December 2020

Table 1. The key manufacturer's specifications for the sensors used in different experiments: The unavailable fields are left blank. Data sheet for each sensor packages are available at iMet XQ2 (iMet-XQ2 , 2020), iMet XQ1 (iMet-XQ1 , 2020), and nimbus-pth (nimbus-pth , 2020)

		XQ2 **(iMet XQ2)**	**XQ1** **(iMet XQ1)**	nimbus-pth **(Custom Built)**
Temperature	Type	Bead Thermistor	Bead Thermistor	Bead Thermistor
	Range	−90 to 50 °C	−95 to 50 °C	−40 to 100 °C
	Response Time	1s @ 5 m/s	2 s	
	Resolution	0.01 °C	0.01 °C	0.01 °C
	Accuracy	±0.3 °C	±0.3 °C	
Humidity	Type	Capacitive	Capacitive	Capacitive
	Range	0–100% RH	0–100% RH	0–100%
	Response Time	@ 25 °C, 0.6 s @ 5 °C, 5.2 s @ −10 °C, 10.9 s	5 s @ 1 m/s velocity	8 s
	Resolution	0.1% RH	0.7% RH	0.01% RH
	Accuracy	±5% RH	±5% RH	±2%

position, velocity, and attitude, through a serial interface. Additionally, a mobile application allows a user to plan and deploy a flight trajectory, and the remote controller allows intervention from the user at any point.

2.2 Sensors:

Specifications of the temperature-humidity (TH) sensors recorded in the dataset are described in Table 1. Every UAS flight used one *iMet XQ2* from InterMet Systems (Grand Rapids, MI, USA) as the primary TH sensor. The *XQ2* is a self-contained sensor package designed for UASs to measure atmospheric pressure, temperature, and relative humidity. It is also equipped with built-in GPS, and an internal data logger along with a rechargeable battery. A serial interface provides access to the logs, or real-time observations produced by the sensor at 1Hz. The internal data-logger was only used as backup and is not part of this dataset. Data included in the dataset are collected through the DAQ using the serial interface. Some UAS flights feature an older version of this sensor, called *iMet XQ1*, as the secondary backup sensor.

Some flights also use a *nimbus-pth* as the secondary sensor, which is a pressure, temperature and humidity sensor we designed and built. Several *nimbus-pth* can be stacked as nodes, and in some data files two of them might be present. In such cases, one of them is aspirated inside our sensor housing, and other one sits directly underneath the UAS in a traditional non-aspirated configuration. In the data files, first two sensors are shielded and aspirated inside the housing, and the third sensor (when available) is in traditional non-aspirated configuration.

https://doi.org/10.5194/essd-2020-374
Preprint. Discussion started: 17 December 2020

2.3 Sensor Housing

The sensor housing is designed to meet or exceed sensor placement requirements, such as constant aspiration for the sensors, shielding from the solar radiation and other indirect heat sources. The housing draws air passively by exploiting the pressure differential between the region just above a propeller and the region just beyond the rotor wash. The airflow through the housing is always maintained as long as the propellers are spinning, and provides a consistent aspiration for the sensors. The inlet and outlet of the housing are shaped as a cone to provide high speed airflow across the housing tube with small pressure difference between the two ends. Additional design considerations are made to ensure that the flow is consistent, and provides airflow $\geq$ 5m/s across the sensors even at the lowest propeller speeds.

The housing is also designed to be modular, printed entirely using a 3D printer, and has an easy screw-in assembly. Impact of the housing on the UAS's stability and flight time is minimal. Further details and the full schematic of the housing and the evaluation can be found in our previous work (Islam *et al.* , 2019).

2.4 Data acquisition:

Data are collected using a data acquisition (DAQ) system made of a compact single-board computer, Odroid XU4 (Odroid , 2019) running a linux operating system. Odroid runs the robot operating system (ROS) (ROS , 2019) that communicates with the serial devices through the USB port of the Odroid. ROS facilitates collecting many different sensor data independently at their own output frequency; recording the timestamp for when data were generated and when they are received by ROS. ROS interfaces the collection of all available devices even in the case of a single device fail. Synchronization of the data can either be done at runtime or in the post-processing. In our case, it is done in the post-processing using MATLAB.

Odroid was connected with a ground computer using wireless 2.4 GHz XBee radios for operation of DAQ, debugging and periodic checks on the data. The data collected by the DAQ were retrieved using an ethernet connection.

Temperature-humidity sensors connect over serial with ROS to send periodic updates of the observations. UAS's autopilot also interface with ROS to provide updates of position, velocity, altitude, attitude etc. which are also recorded to spatially and temporally synchronize the observation.

2.5 UAS Sensor Mounting Configuration and Payload:

As mentioned in the subsection 2.2, the primary sensor is the *iMet XQ2*, and its data are recorded on the dataset with a header underscore _1 (e.g., Temperature_1, Humidity_1, Pressure_1). Other sensor data headers are followed with _2 and _3 when available. Sensor_2 is shielded inside the sensor housing, however sensor_3 is placed under the UAS in a traditional configuration without aspiration. Specific placement of the sensors on the UAS used in the data collection are described below.

UAS platform M600P1

One XQ2 (sensor_1) is placed inside the left sensor housing, and one XQ1 (sensor_2) is on a identical right sensor housing. The alternative setup used in some experiments replaces XQ1 with nimbus-pth (sensor_2) inside the right sensor housing (sensor

https://doi.org/10.5194/essd-2020-374
Preprint. Discussion started: 17 December 2020

Open Access Earth System Science Data Discussions

names are also listed in metadata as data source). An additional nimbus-pth (sensor_3) is also placed under the body of the UAS without housing whenever nimbus-pth is included in measurements.

UAS platform M600P2

One XQ2 (sensor_1) is mounted inside the left sensor housing, one nimbus-pth (sensor_2) is mounted inside the right sensor sensor housing, and an additional nimbus-pth (sensor_3) is placed under the body of the UAS without a housing. This form of sensor placement facilitates an evaluation between the sensor placed inside the housing versus under the body of the UAS without housing. It also allows comparison of the sensor mounted on the opposite ends of the UAS. Having secondary sensors also provides a fail-safe when the primary sensors fail - such as the case on XQ2 humidity sensors on 17 July, 2018 data.

The UAS's payload during the experiments were $\sim$1.8 kg. Sensor housing with support structure and sensor is $2\times\sim$720 gm, onboard computer is $140gm$, misc cables, screws etc. are approx. $200gm$. UAS flight endurance was 20–25 min with the payload.

3 Flight locations, and strategies

3.1 Flight locations

We conducted flights in locations designated as Golf, Gamma, Leach, India, Charlie in LAPSE-RATE flight campaign. GPS coordinates of the locations are provided in Table 2 and illustrated in a terrain map in Figure 2.

Table 2. Latitude, longitude, and mean sea level (MSL) altitude of operation locations in World Geodetic System 84 (WGS 84) decimal degrees.

Location	Latitude	Longitude	Altitude (MSL)
Golf	37.626963	-105.820028	2298 m
Gamma	37.893536	-105.716137	2329 m
Leach Airfield	37.784560	-106.044552	2316 m
India	38.051294	-106.102885	2332 m
Charlie	38.052690	-106.087414	2329 m

3.2 Flight strategies

Table 3 shows the distribution of UASs deployed by UNL by date and time and mission objectives.

On July 14, 2018, the mission objective was to compare both of the systems against a reference point, the MURC tower (de Boer *et al.* , 2020), to calibrate and validate the sensor observations. One flight for each system was conducted where the UAS ascended to the height of MURC tower (15.2m) and hovered for 10 minutes. After that, the UAS ascended to 120m at 1m/s, hovered for 30 seconds, and descended at the same speed to land. This mission was performed in collaboration with

https://doi.org/10.5194/essd-2020-374
Preprint. Discussion started: 17 December 2020

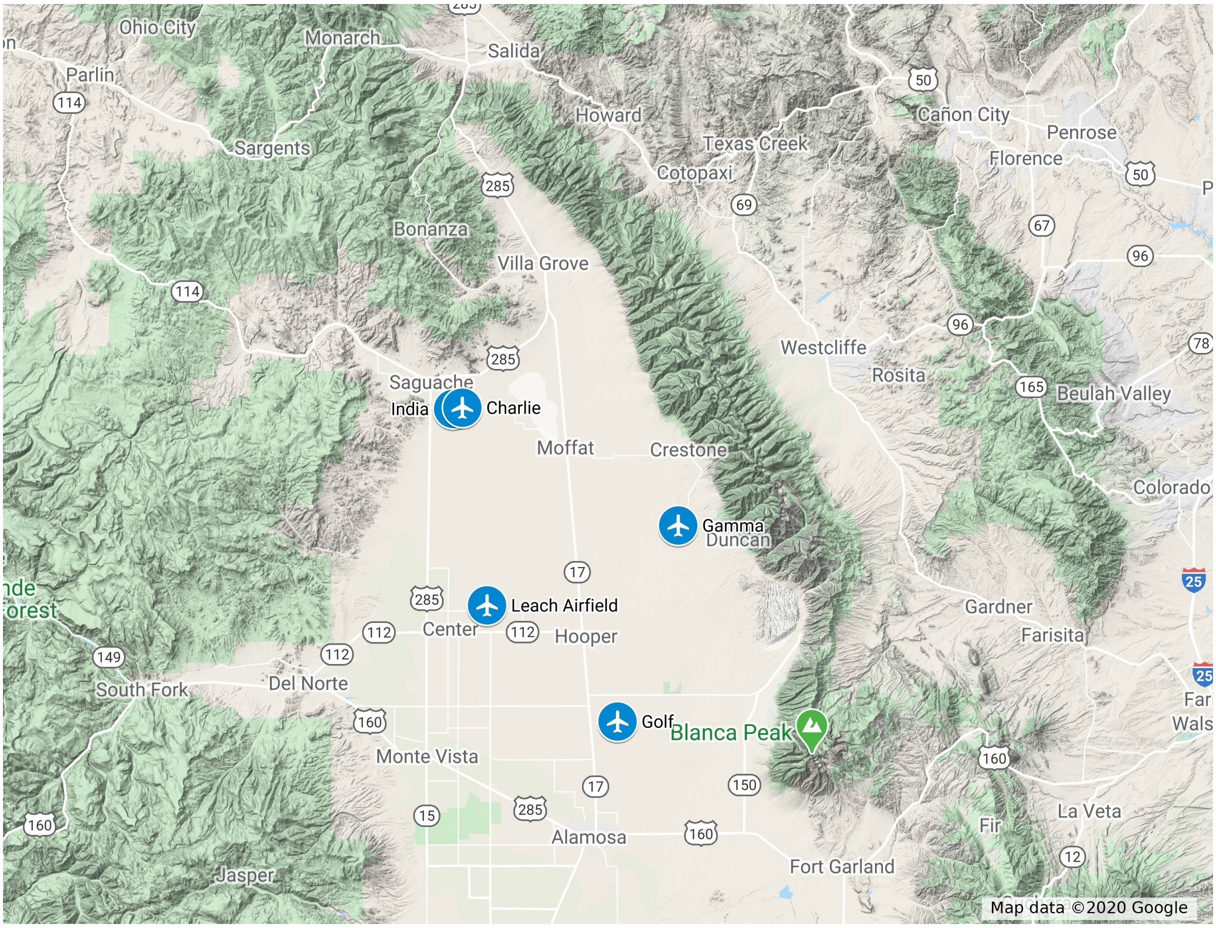

Figure 2. Flight locations overlaid on the terrain map. Map data © Google 2020

all participating teams at the LAPSE-RATE campaign to provide measurement intercomparison between platforms from all teams (Barbieri *et al.* , 2019). The data for the MURC tower and other teams are located in the Zenodo community for LAPSE-RATE at (LAPSE-RATE Community , 2020).

On July 15, 2018, the mission objective of the day was convection initiation (CI). Vertical profiling flights were conducted up to 500m altitude at 1m/s ascent/descent speed in Golf and Gamma location. Flights were planned to be at every 30 minutes to allow recharge of the UAS batteries while cycling through multiple sets of batteries. At Golf, the weather was slightly cloudy in the morning; clear throughout the day; very windy conditions existed for the last few flights. At Gamma, the weather was clear and windy in the morning, and slightly cloudy for the last half of the flights.

On July 16, 2018, the scheduled mission objective was also CI with flights at the same locations. Flights were limited to 120m altitude at 1.5m/s ascent/descent speed due to Notice to Airman (NOTAM) not being active for the day. Due to reduced altitude, more flights could be conducted with available batteries. As such, flights were conducted every 15 minutes. At Golf,

https://doi.org/10.5194/essd-2020-374
Preprint. Discussion started: 17 December 2020

Table 3. UAS locations and mission objectives. Calibration flight (CLF), Boundary layer transition (BLT), Convection initiation (CI), Cold air drainage flow (CDF)

				Location				
Date and Time	Objective	No. of Flight	Max. Altitude	Golf	Gamma	Leach	India	Charlie
July 14, 2018 (17:17-17:33 MDT)	CLF	2	120m			M600P2, M600P1		
July 15, 2018 (9:00-15:15 MDT)	CI	19	500m	M600P2	M600P1			
July 16, 2018 (8:00-14:30 MDT)	CI	47	120m	M600P2	M600P1			
July 17, 2019 (7:00-9:00 MDT)	BLT	18	100m			M600P2, M600P1		
July 18, 2019 (7:00-14:30 MDT)	CI	43	120m	M600P2	M600P1			
July 19, 2019 (5:30-11:00 MDT)	CDF	43	500m				M600P2	M600P1

the weather started slightly cloudy, and then clear through out the day. At Gamma, the weather was clear throughout the day, with partly cloudy condition for the last few flights.

On July 17, 2018, the scheduled missions were for boundary layer transition (BLT). The early morning experiments, before sunrise, help validate the sensor housing reading since the measurement error from the downwash is more easily detected in stable versus well-mixed conditions. We conducted simultaneous flights for both UAS with six vertical profile and 3 horizontal profile at various UAS movement speeds. The sky was cloudy throughout all the flights.

On July 18, 2018, the scheduled mission was for CI. Flights were conducted up to 500m altitude at 1.5m/s ascent/descent speed at both Golf and Gamma locations. Flights were generally conducted every 30 minutes. At the conclusion of the day, ten additional 150 m altitude flights were performed at the Golf location at various ascent/descent speed to study the effect of UAS movement speed on temperature and humidity observations. At both location, sky was clear for first half of the flights, and partly cloudy for the second half.

On July 19, 2018, the mission objective was cold drainage flow. UASs were placed at the Charlie and India locations for this mission. Flights were performed starting before sunrise at maximum altitudes up to 350m at 1.5m/s ascent/descent speed. Flights were scheduled for every 15 minutes. At both locations, the sky was cloudy before sunrise but clear afterwards.

https://doi.org/10.5194/essd-2020-374
Preprint. Discussion started: 17 December 2020

4 Data processing and quality control

Data are recorded from individual sensors and UAS flight controller as they arrive to the DAQ as described earlier. The recorded data are then processed in MATLAB to synchronize using zero-order-hold method to create a single output file. We used a discrete sample time of 1 second for zero-order-hold to match the output rate of primary sensors. Invalid or missing data are replaced with -9999.9 wherever the sensor data are unavailable to the DAQ.

We note that the humidity sensor of the XQ2 on some flights for July 17, 2018 was saturated at 100% in one of the UAS (M600P1) and are not usable; secondary sensor measurements should be used to replace these data. Also, humidity readings from nimbus-pth have sensitivity issues; although it displays a similar trend as the other sensors it does not capture the whole range of observation and will need further calibration.

No other processing was done on the data such as sensor response correction, bias correction, etc. File naming convention and explanation of the data fields can be found in the read-me file of Zenodo data repository.

5 Special topics of interest

The following are special topics of interest that can be studied from the dataset. Our analysis that focused on these topics can be found in our previous work (Islam *et al.* , 2019).

Calibration:

Data from July 14, 2018 can be used with MURC data available at Zenodo to obtain reference for calibration (de Boer *et al.* , 2020). Our previous paper (Islam *et al.* , 2019) discusses the deviation of our observations with MURC data over a period of 10 minutes. Other work (Barbieri *et al.* , 2019) compares all the different participating platforms along with ours against MURC tower data as well.

Effect of ascent/descent speed:

To study the effect of ascent/descent speed on the sensor readings, 10 flights from M600P2 platform on July 18,2020 starting at 20:21 UTC can be used. Flights were conducted up to 150m altitude with speeds ranging from 1–5m/s ascent speed, and 1–3m/s descent speed. Our analysis on these data can also be found in our paper (Islam *et al.* , 2019).

Detection of Inversion:

To study the sensor performance within an inversion layer, the first six flight from each platform can be used from July 17, 2020. The speed of flight through the inversion layer ranged from 0.5-5m/s for ascent, and 0.5-3m/s for descent. These data could be used for comparison to the theoretical work of (Houston and Keeler , 2020).

https://doi.org/10.5194/essd-2020-374
Preprint. Discussion started: 17 December 2020

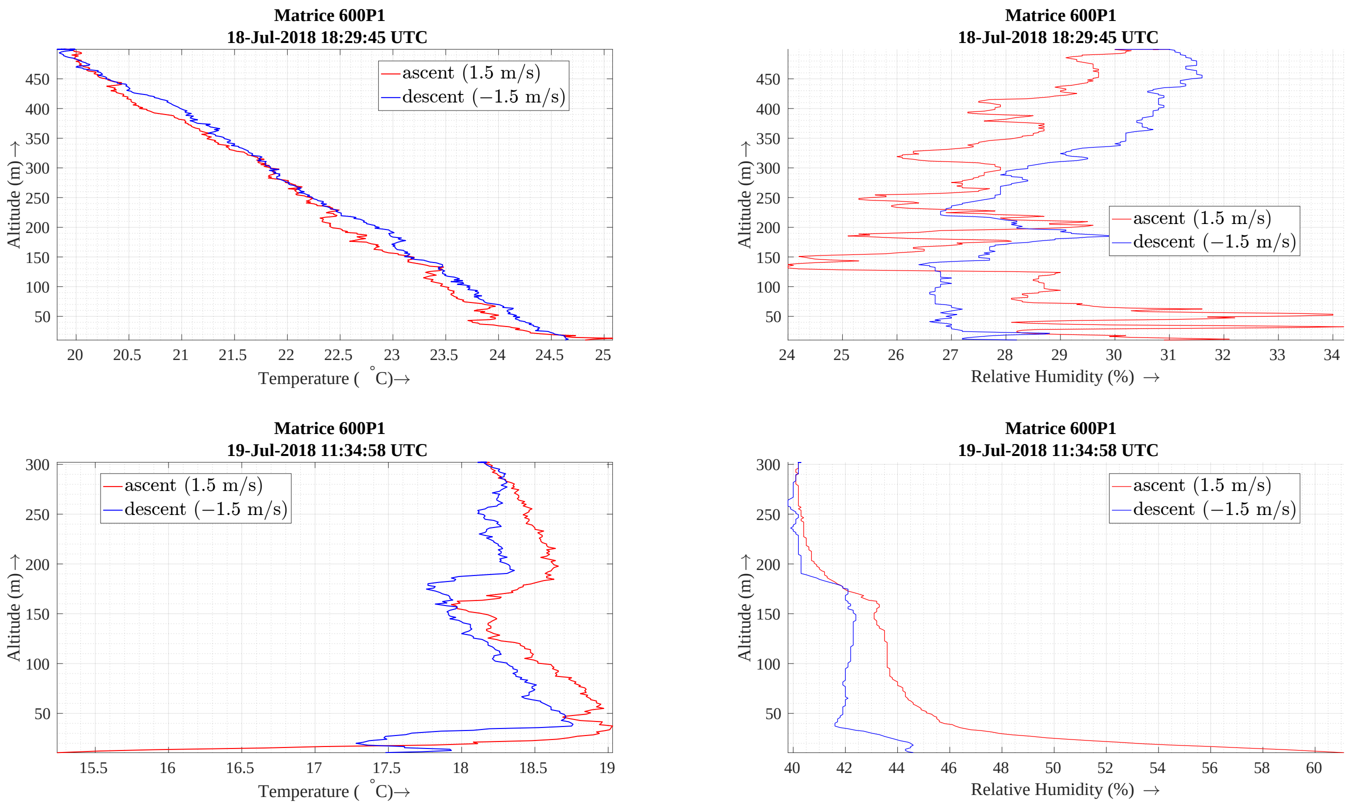

Figure 3. Examples of vertical profile collected using UAS: M600P1

Effect of body-relative wind direction / Horizontal transect:

Data are available to study sensor performance during horizontal transect with different orientations relative to the wind. The last three flights from each platform on July 17, 2020 can be used for this purpose. Horizontal flight speed ranged from 2-10m/s.

6 Examples of collected profile

Figure 3 shows examples of temperature and humidity profiles collected using the M600P1 platform's primary sensor. The top two panels illustrate a 500m profile taken through a well-mixed atmosphere. The bottom two panels in Figure 3 are an example of a profile taken before sunrise through a nocturnal inversion.

Figure 4 and Figure 5 shows primary sensor (XQ2) temperature and relative humidity profiles, respectively, for all the flights conducted between 15-19 July, 2018. The profiles are plotted using artificial offset for clarity. These figures serves the purpose of a quick glance over the dataset and to locate interesting flights for further study.

https://doi.org/10.5194/essd-2020-374
Preprint. Discussion started: 17 December 2020

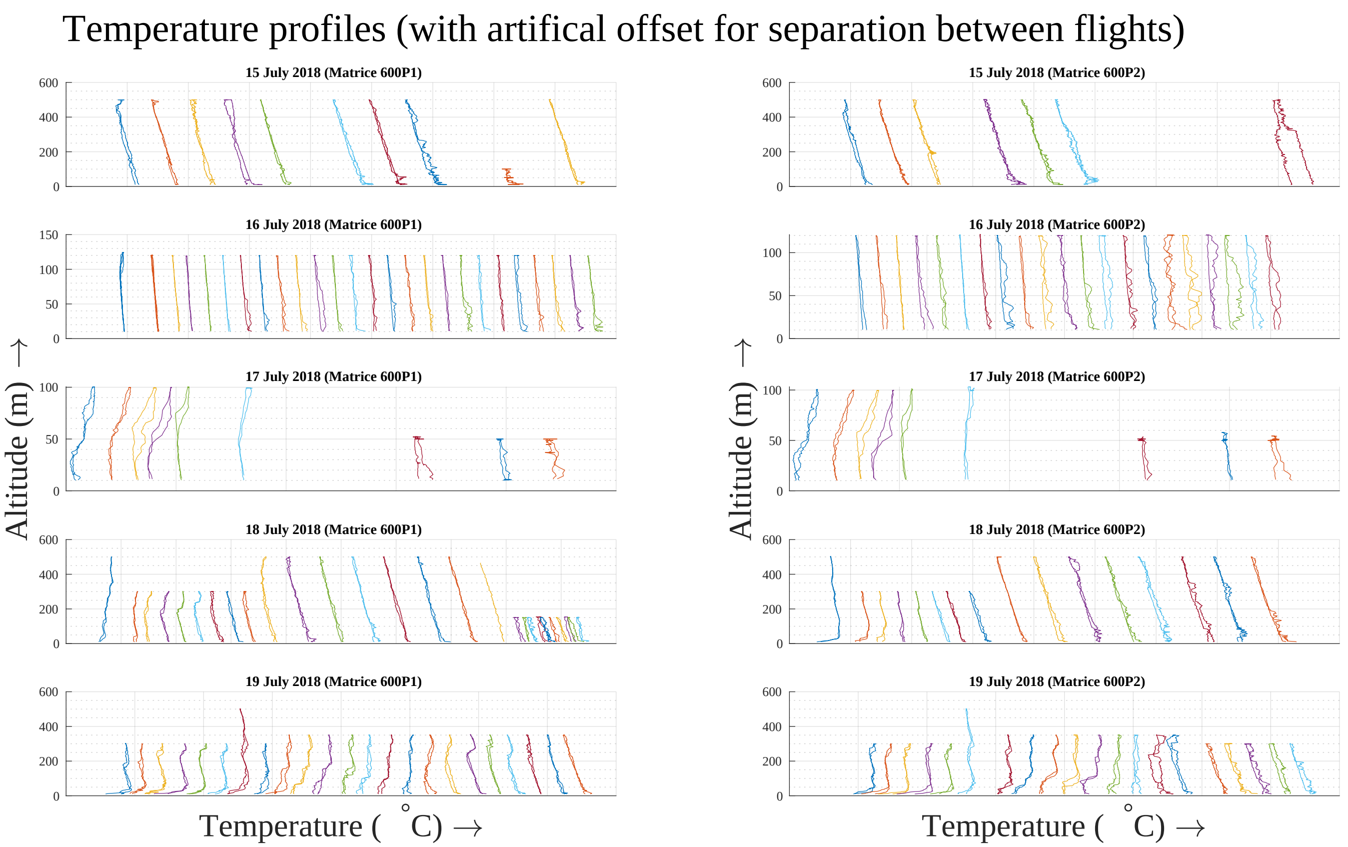

Figure 4. Temperature profile from the primary sensor (XQ2) in all flights from 15-19 July, 2018

7 Conclusions

As part of the LAPSE-RATE measurement campaign in July 2018 in San Luis Valley, Colorado, USA, UNL participated in data collection in support of science missions focused on convection initiation, boundary layer transition, and cold air drainage flow. UNL deployed UASs in two location simultaneously for each mission. A total of 172 flights were conducted up to a maximum 500m altitude above ground level (AGL). All data are available for open access at Zenodo data repository (Islam *et al.* , 2020).

8 Data availability

Dataset is available at Zenodo with Creative commons license. https://doi.org/10.5281/zenodo.4306086 (Islam *et al.* , 2020).

Author contributions. Authors contributed equally.

https://doi.org/10.5194/essd-2020-374
Preprint. Discussion started: 17 December 2020

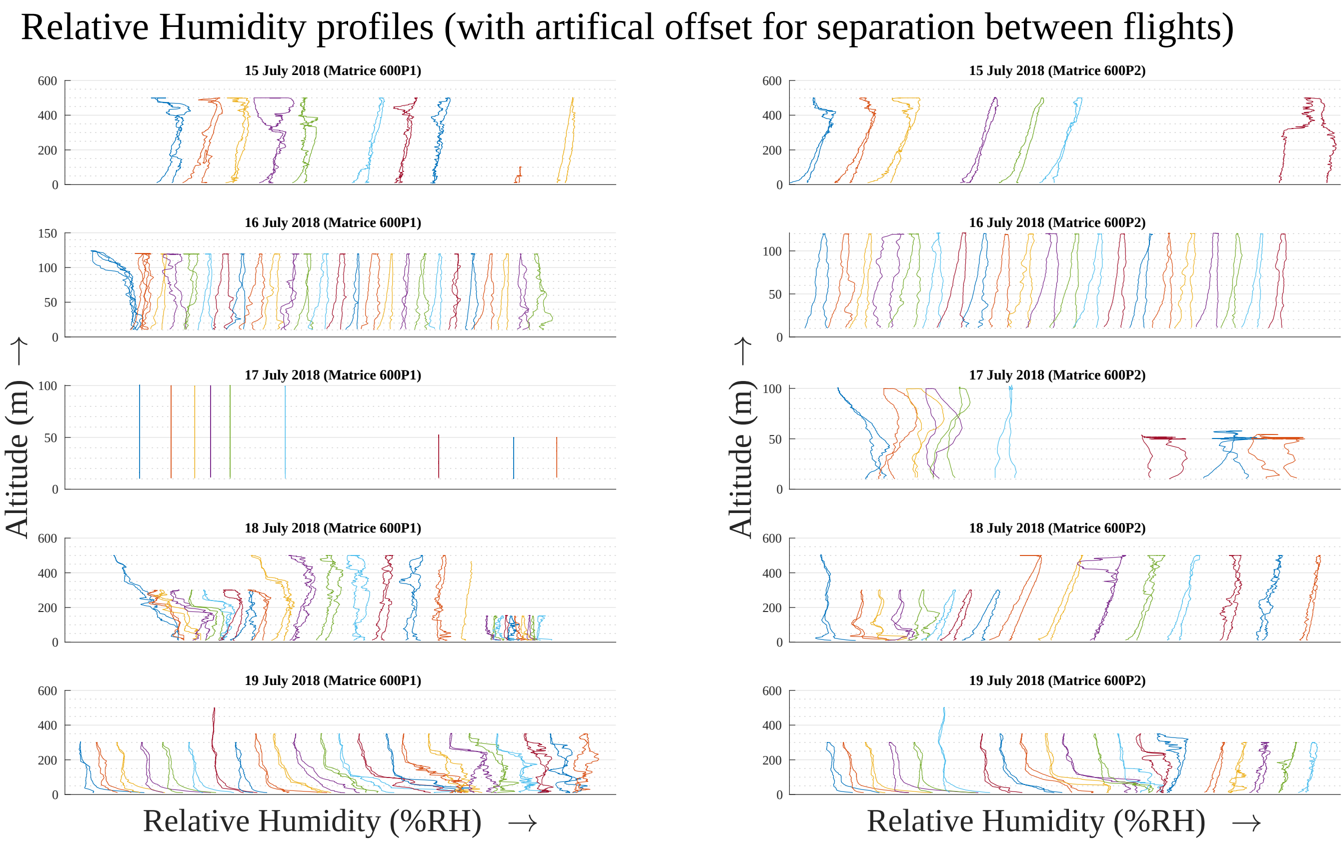

Figure 5. Relative humidity profile from the primary sensor (XQ2) in all flights from 15-19 July, 2018

Competing interests. The authors declare no competing interests. The funders had no role in the design of the study; in the collection, analyses, or interpretation of the data; in the writing of the manuscript; or in the decision to publish the results.

Acknowledgements. This work was partially supported by NSF IIA-1539070, IIS-1638099, IIS-1925052, IIS-1925368, and USDA-NIFA 2017-67021-25924. Limited general support for LAPSE-RATE was provided by the US National Science Foundation (AGS 1807199) and the US Department of Energy (DE-SC0018985) in the form of travel support for early career participants. Support for the planning and execution of the campaign was provided by the NOAA Physical Sciences Division and NOAA UAS Program.

We thank Jason Finnegan and Amy Guo for their help with data collection during the LAPSE-RATE flight campaign. We would like to thank Dr. Sean Waugh and the National Severe Storms Laboratory for the radiosonde data. We also thank S. Borenstein and C. Dixon for their help with the MURC operations.

References

Islam, A., Houston, A., Shankar, A., and Detweiler, C.: University of Nebraska-Lincoln Unmanned Aerial System observations from LAPSE-RATE (Version v1) [Data set], Zenodo, http://doi.org/10.5281/zenodo.4306086, 2020.

Islam, A., Houston, A.L., Shankar, A. and Detweiler, C.,: Design and evaluation of sensor housing for boundary layer profiling using multirotors, Sensors, 19(11), p.2481, https://doi.org/10.3390/s19112481, 2019.

Elston, J., Argrow, B., Stachura, M., Weibel, D., Lawrence, D., and Pope, D.: Overview of small fixed-wing unmanned aircraft for meteorological sampling, J. Atmos. Ocean. Technol., 32, 97–115, https://doi.org/10.1175/JTECH-D-13-00236.1, 2015.

Bonin, T., Chilson, P., Zielke, B., and Fedorovich, E.: Observations of the early evening boundary-layer transition using a small unmanned aerial system, Bound. Layer Meteorol., 146, 119–132, https://doi.org/10.1007/s10546-012-9760-3, 2013.

Houston, A.L., Argrow, B., Elston, J., Lahowetz, J., Frew, E.W., and Kennedy, P.C.: The collaborative Colorado–Nebraska unmanned aircraft system experiment, Bull. Am. Meteorol. Soc., 93, 39–54, https://doi.org/10.1175/2011BAMS3073.1, 2012.

Jacob, J., Chilson, P., Houston, A., and Smith, S.: Considerations for atmospheric measurements with small unmanned aircraft systems, Atmosphere, 9, 252, https://doi.org/10.3390/atmos9070252, 2018.

Houston, A., Chilson, P., Islam, A., Shankar, A., Greene, B., Segales, A., and Detweiler, C.: PTH Sensor Siting on Rotary-Wing UAS, in: Proceedings of the 19th AMS Symposium on Meteorological Observation and Instrumentation, Austin, TX, USA, 7–11 January 2018, 6.7, 2018.

DJI Matrice 600 Pro: https://www.dji.com/matrice600-pro/info#specs, last access: 16 December 2020.

Odroid XU4: https://magazine.odroid.com/odroid-xu4, last access: 16 December 2020.

Robot Operating System (ROS): http://www.ros.org/, last access: 16 December 2020.

Mobile UAS Research Collaboratory (MURC): https://www.colorado.edu/iriss/content/our-capabilities/murc last access: 16 December 2020.

Barbieri, L., Kral, S.T., Bailey, S.C.C., Frazier, A.E., Jacob, J.D., Reuder, J., Brus, D., Chilson, P.B., Crick, C., Detweiler, C., Doddi, A., Elston, J., Foroutan, H., González-Rocha, J., Greene, B.R., Guzman, M.I., Houston, A.L., Islam, A., Kemppinen, O., Lawrence, D., Pillar-Little, E.A., Ross, S.D., Sama, M.P., Schmale, D.G., Schuyler, T.J., Shankar, A., Smith, S.W., Waugh, S., Dixon, C., Borenstein, S., and de Boer, G.: Intercomparison of Small Unmanned Aircraft System (sUAS) Measurements for Atmospheric Science during the LAPSE-RATE Campaign, Sensors, 19, 2179, https://doi.org/10.3390/s19092179, 2019.

Lower Atmospheric Profiling Studies at Elevation - a Remotely-piloted Aircraft Team Experiment (LAPSE-RATE): https://zenodo.org/communities/lapse-rate/, last access: 16 December 2020.

de Boer, G., Borenstein, S., Dixon, C., and Argrow, B.: University of Colorado MURC Observations from LAPSE-RATE (Version 2) [Data set], Zenodo, http://doi.org/10.5281/zenodo.3875493, 2020.

de Boer, G., Waugh, S., Erwin, A., Borenstein, S., Dixon, C., Shanti, W., Houston, A., and Argrow, B.: Measurements from mobile surface vehicles during LAPSE-RATE, Earth Syst. Sci. Data Discuss., https://doi.org/10.5194/essd-2020-173, in review, 2020.

Houston, A. L., and Keeler, J. M.: Sounding Characteristics that Yield Significant Convective Inhibition Errors due to Ascent Rate and Sensor Response of In Situ Profiling Systems, J. Atmos. Oceanic Technol., 37, 1163–1172, https://doi.org/10.1175/JTECH-D-19-0191.1, 2020.

Villa, T.F., Salimi, F., Morton, K., Morawska, L., and Gonzalez, F.: Development and validation of a UAV based system for air pollution measurements, Sensors, 16, 2202, https://doi.org/10.3390/s16122202, 2016.

Prudden, S., Fisher, A., Mohamed, A., and Watkins, S.: A flying anemometer quadrotor: Part 1, in: Proceedings of the International Micro Air Vehicle Conference (IMAV 2016), Beijing, China, 17–21 October 2016, 17–21, 2016.

https://doi.org/10.5194/essd-2020-374
Preprint. Discussion started: 17 December 2020

Greene, B.R., Segales, A.R., Waugh, S., Duthoit, S., and Chilson, P.B.: Considerations for temperature sensor placement on rotary-wing unmanned aircraft systems, Atmos. Meas. Tech., 11, 5519–5530, https://doi.org/10.5194/amt-11-5519-2018, 2018.

Houston, A.L., and Keeler, J.M.: The impact of sensor response and airspeed on the representation of the convective boundary layer and airmass boundaries by small unmanned aircraft systems, J. Atmos. Ocean. Technol., 35, 1687–1699, https://doi.org/10.1175/JTECH-D-18-0019.1, 2018.

Ventura Diaz, P., and Yoon, S.: High-fidelity computational aerodynamics of multi-rotor unmanned aerial vehicles, in: Proceedings of the 2018 AIAA Aerospace Sciences Meeting, Kissimmee, FL, USA, 8–12 January 2018, p. 1266, 2018.

Yoon, S., Ventura Diaz, P., Boyd, D.D., Chan, W.M., and Theodore, C.R.: Computational aerodynamic modeling of small quadcopter vehicles, in: Proceedings of the 73rd Annual AHS International Forum and Technology Display 2017, Fort Worth, TX, USA, 9–11 May 2017, 2017.

iMet-XQ2 UAV Sensor: https://www.intermetsystems.com/ee/pdf/202021_iMet-XQ2_171207.pdf, last access: 2 December 2020.

iMet-XQ1 UAV Sensor: https://www.intermetsystems.com/ee/pdf/202020_iMet-XQ_161005.pdf, last access: 2 December 2020.

nimbus-pth Temperature-Humidity sensor: Temperature sensor data sheet, https://media.digikey.com/pdf/Data%20Sheets/Littelfuse%20PDFs/GP103J4F.pdf, last access: 4 December 2020. Humidity sensor data sheet, https://www.mouser.com/datasheet/2/682/Sensirion_Humidity_Sensors_SHT3x_Datasheet_digital-971521.pdf, last access: 4 December 2020.